

institute in Theoretical Physics, Waltham, Massachusetts (Gordon and Breach, New York, 1966).

¹¹M. L. Goldberger and K. M. Watson, Collision Theory (John Wiley & Sons, New York, 1964).

¹²K. M. Watson, *Phys. Rev.* **89**, 575 (1953); **105**, 1388 (1957).

¹³A. Ahmadzadeh and J. A. Tjon, *Phys. Rev.* **139**, B1085 (1965); T. Osborn and H. P. Noyes, *Phys. Rev. Letters* **17**, 215 (1966); see also R. Balian and E. Brézin, *Nuovo Cimento* (to be published).

¹⁴The expression of Coulomb potential $V_l^{(i)}$, and the normalization of the two-body amplitude $t_l^{(i)}$, are different from those in Paper I by a sign. These changes in sign make them agree with the convention adopted in atomic physics. The Coulomb potential $V_l^{(i)}$ is attractive if $Z_i = -|Z_i|$ and repulsive if $Z_i = |Z_i|$.

¹⁵It should be noted that the representation for $t_l(p, p'; E)$ given by Eqs. (2.33) and (2.34) is not limited to Coulomb potentials. This representation is in general valid for any central-field potential $V_l(p, p')$. It should also be noted that this representation is not a simple expansion in terms of the set of eigenfunctions $\{\psi_n\}$ of Eq. (2.25) with $V_l(p, p')$ potential, since the coefficients depend explicitly on p and p' .

¹⁶Since Sturmian functions form a complete set for an arbitrary negative energy, one may, in principle,

utilize the completeness property for expansion to deal with problems at energies lying above the three-body break-up threshold.

¹⁷J. C. Y. Chen and T. Ishihara, *Phys. Rev.* (to be published). Some of the results were reported at the American Physical Society 1968 Winter Meeting in San Diego by T. Ishihara and J. C. Y. Chen, *Bull. Am. Phys. Soc.* **13**, 1655 (1968).

¹⁸If the initial and final two-body bound states were not properly factored out due to, for example, improper normalization of these wave functions, the collision amplitude is then determined only within a multiplicative constant c . Care must be exercised to remove this constant. A simple procedure for determining such a multiplicative constant is to write the collision amplitudes in terms of eigenphase shifts and connecting parameters [see Eqs. (3.23) to (3.26)], including explicitly the multiplicative constants. The constants as well as eigenphase shifts and connecting parameters can then be determined by solving this set of equations.

¹⁹E. P. Wigner, Group Theory (Academic Press Inc., New York, 1959); see also M. Jacob and G. C. Wick, *Ann. Phys. (N. Y.)* **7**, 404 (1959)

²⁰A. Temkin and J. C. Lamkin, *Phys. Rev.* **121**, 788 (1961).

Studies of Negative-Ion-Molecule Reactions in the Energy Region from 0 to 3 eV[†]

J. A. D. Stockdale, R. N. Compton, and P. W. Reinhardt

Health Physics Division, Oak Ridge National Laboratory, Oak Ridge, Tennessee 37830

(Received 28 April 1969)

A modulated retarding-potential-difference technique has been used to define the energy width of an electron beam located in the source region of a time-of-flight mass spectrometer. Negative ions with energies in the region 0–3 eV are produced by dissociative electron attachment to gas molecules in this source and are permitted to react for a controlled continuously variable length of time with neutral molecules to produce secondary negative-ion products. From the observed time development of the reactions, the reaction rate constant may be obtained, and the cross section then calculated if the primary-ion velocity is known. Results are presented for the reactions $O^- + NO_2 \rightarrow NO_2^- + O$, $H^- + H_2O \rightarrow OH^- + H_2$, and $D^- + D_2O \rightarrow OD^- + D_2$ at a number of primary ion energies, and for the reactions $O^- + N_2O \rightarrow NO^- + NO$, $HCOO^- + SF_6 \rightarrow SF_5^{*-} + (HCOOF)$, and $SF_6^- + HCl \rightarrow F_2Cl^- + (SF_4H)$ at single energy points.

I. INTRODUCTION

It has proved difficult to measure ion-molecule or charge-exchange cross sections as functions of the primary-ion energy in the region below a few eV. Drift-tube techniques¹ are confined in practice to energies ≤ 0.1 eV and yield cross sections averaged over a range of ion energies. The flowing afterglow technique² is limited to thermal

energies and collisional heating of the target neutrals. The components of the afterglow may make it difficult to compare directly rate constants obtained in this way with those from beam methods. The latter³ have yielded most of the information which exists on the variation of cross sections with energy but are confined⁴ to the energy region above a few eV because of difficulties in obtaining adequate energy resolution and beam intensity at

low beam energies. The merging-beams technique⁵ offers a solution to the problem in principle, but in this method, it is necessary to obtain a neutral beam at relatively high laboratory energy (a few keV) for merging with the charged beam at comparable energy. Since the neutrals are usually produced by accelerating a charged beam to the required energy E and then passing it through a neutralizing gas cell, the formation of a component of excited neutrals is quite likely. There is good evidence⁶ that reaction cross sections are strongly dependent on the state of excitation of the reactants.

Many charge-exchange and ion-molecule reactions have been observed in studies in which the ion source region of a mass spectrometer has been used as the reaction chamber.⁷ In most of this work, the phenomenological cross section Q of the reaction has been obtained as a function of the electric field V/d required to repel the ions into the mass analysis system.⁷ The microscopic cross section σ is related to Q through

$$Q = \frac{1}{V} \int_0^V \sigma(E) dE. \quad (1)$$

Perhaps the chief criticism which can be made of this method lies in the fact that σ , not Q is the quantity of interest for comparison with available theory.

It is the purpose of this paper to present some measurements of negative-ion reaction rates k and cross sections σ which have been made in the energy region from 0 to 3 eV by a mass spectrometer method which avoids most of the difficulties mentioned above.

II. EXPERIMENTAL METHOD

A. Sketch of Method

A preliminary account of the method has been published.⁸ Dillard and Franklin⁹ and Dillard, Franklin, and Seitz¹⁰ have independently described some similar work but have not reported any measurements of σ as a function of E .

The reactions proceed in the source region of a Bendix Model 14-206 time-of-flight mass spectrometer. This apparatus, including the retarding-potential-difference (RPD) electron-beam ionizer has been described in detail elsewhere.¹¹ Primary negative ions A^- were produced by dissociative electron attachment to the target gas molecules AB



which results in A^- acquiring the most probable energy

$$E_0(A^-) = (1 - \beta)[E_e - (D - EA)], \quad (3)$$

where β is the ratio of the mass of A^- to the mass of AB , E_e is the electron beam energy, D the dissociation energy of the $A-B$ bond, and EA the electron affinity of A . Because of the normal range of electron affinities and bond strengths and the values of E_e at which dissociative attachment resonances are found,¹² E_0 falls in the region between 0 and 3 eV. Equation (3) does not hold if either of the fragments A^- or B are rotationally, vibrationally, or electronically excited. In this case, separate measurements must be made to obtain E_0 . To date, the most comprehensive and accurate data have been obtained from measurements of ion current against retarding voltage from which the derivative yields the ion energy distribution,¹³ though Franklin, Hierl, and Whan¹⁴ have also described a time-of-flight method which yields the component of ion kinetic energy along the axis of the flight tube.

The primary negative ions A^- were produced by a pulse of electrons of duration set from 50 nsec to ~ 1 μ sec depending on the rate of the reaction being studied. The gate pulse width should be kept short compared to the "period" $(nk)^{-1}$ of the reaction [see Eq. (4)]. After this short production pulse, the primary ions were free to react with whatever target gas molecules were present, for a time period of t sec, until a fast rising extraction pulse was applied to terminate the reaction and repel both primary and product ions into the flight tube. The 200-V/cm extraction pulse rose to half-maximum in ~ 3 nsec. The source region of the mass spectrometer was kept field free during production of the primary ions by electron impact as well as during the reaction time t .

During the reaction time, before the primary ions begin to leave the interaction region, because of their initial kinetic energy the variation of the secondary-ion current $[i_s]$ with reaction time t is given by

$$[i_s]_t = [i_p]_{t=0} (1 - e^{-nkt}), \quad (4)$$

where $[i_s]_t$ is the product-ion current at time t , $[i_p]_{t=0}$ is the primary-ion current at time $t=0$, n is the number density of the target gas molecules, and k is the rate constant of the reaction at a given primary-ion energy E . The slope of a plot of $-\ln(1 - [i_s]_t/[i_p]_{t=0})$ against t is equal to nk . Therefore, if the target gas pressure is known, k may be obtained, and since

$$k = \sigma v, \quad (5)$$

σ may be calculated if v , the primary-ion velocity, is known [e.g., from Eq. (3)]. Production of pri-

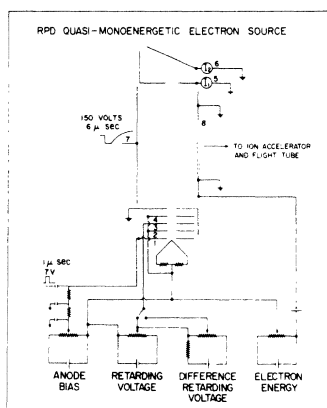


FIG. 1. Schematic diagram of the retarding-potential-difference electron gun and ion source.

primary ions from a number of dissociative attachment resonances yields information on the variation of σ with E .

The effect of the extraction pulse on the measured rate constants has been considered previously⁸ and is thought to be negligible in the work reported here.

B. Ion Energy Resolution

The ion energy resolution is largely determined by the electron beam energy resolution. Quasi-monoenergetic electrons were obtained by application of the RPD technique of Fox, Hickam, Grove, and Kjeldaa.¹⁵ For most of the measurements reported here, a modulated retarding voltage, a sine wave, or square wave of amplitude 0.1 or 0.2 V at a frequency of 22 Hz, was applied to the retarder grid 3 of the electron gun shown in Fig. 1 in place of the usual constant difference voltage. Electrons within this modulated band produced correspondingly modulated primary ions by dissociative attachment and these through ion-molecule reactions or charge exchanges produced in turn a modulated component in the secondary-ion current. The ion current corresponding to a given mass was obtained by applying a fast (~ 40 nsec) pickoff gate pulse, to one of the collector anodes of the electron multiplier detector located at the end of the flight tube. This current was amplified and the modulated component recovered by phase sensitive detection and demodulation by a PAR model HR-8 lock-in amplifier which also provided the initial electron-beam modulation signal. The demodulated-ion current could be displayed on an X-Y recorder as a function of the electron energy by means of a continuously driven potentiometer which supplied both the X axis of the X-Y recorder and the electron energy bias.

Electron energy resolution of 0.1 eV as measured by the width of the SF_6^- peak at zero elec-

tron energy or by the rising edge of the Cl^-/HCl vertical onset dissociative attachment resonance near 0.8 eV could be obtained in this way. However, this resolution could not always be utilized because of the necessity of producing enough primary ions for the secondary currents to be detected.

During the period between application of the electron gate pulse and depletion of the primary-ion current by escape of ions from the interaction region or by significant loss through ion-molecule reaction, the energy distribution of primary ions is given by the convolution of the dissociative attachment cross section $\sigma_{da}(E_e)$, the electron energy distribution $N(E_e)$, and the energy spread due to thermal motion of the molecules prior to attachment. If the electron energy is set at the peak of a dissociative attachment resonance, the product of the first two factors results in a distribution narrower than the electron energy distribution.

Figure 2 illustrates this for a broad electron energy distribution and the $\text{H}^-/\text{H}_2\text{O}$ dissociative attachment resonance at 6.5 eV electron energy. The last factor has been considered by Chantry and Schulz¹⁶ who have shown that for the case of dissociative attachment of monoenergetic electrons to a diatomic molecule in which neither fragment is produced in an electronically excited state, the width at half-maximum of the negative-ion energy distribution $W_{1/2}$ is given by

$$W_{1/2} = (11\beta k T E_0)^{1/2}, \quad (6)$$

where κ is the Boltzmann constant, T is the target gas temperature, and E_0 is the most probable ion energy as given in Eq. (3). For the production of light ions from a relatively heavy parent (e.g., $\text{H}^-/\text{H}_2\text{O}$), this effect is quite small since β is small.

C. Reaction Time Measurement

The electron gate pulse and the ion draw-out pulse could be displayed simultaneously on an oscilloscope and the time difference between them

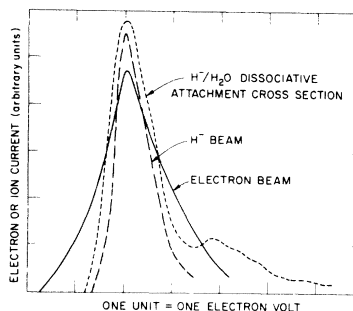


FIG. 2. Convolution of $N(E_e)$ and $\sigma_{DA}(E_e)$ for $\text{H}^-/\text{H}_2\text{O}$ from the 6.5-eV peak.

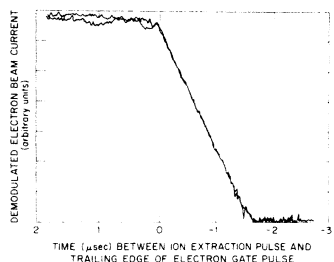


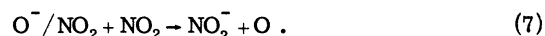
FIG. 3. Modulated component of electron trap current versus time between trailing edge of electron gate pulse and the ion extraction pulse. Two X-Y recorder traces are shown.

measured to an accuracy of better than 5 nsec if necessary. Where the reaction time t under consideration is much greater than the width of the electron gate pulse, a good estimate of t is obtained by taking the interval between the center of the gate pulse and the time the ion draw-out pulse begins to rise. The effect of the finite time width of the electron gate pulse on the shape of the ion current versus reaction time curves may also be allowed for by using the unfolding procedure described in the Appendix. Figure 3 shows two experimental X-Y recorder traces of the cutoff of the modulated component of the electron beam current (as collected on the trap-electrode 6 of Fig. 1) as the electron gate pulse is moved in to coincide with the ion draw-out pulse. The sharpness of the cutoff provided by the meshing of the draw-out pulse and the square-electron beam gate pulse is shown by the straight line dependence of the electron beam current. Differentiation of the curve of Fig. 3 yields back the square-topped electron gate pulse (of width 1.7 μsec in this case).

The position in time of the narrow (~ 40 nsec) pickoff gate pulse, which is applied to the anode of the electron multiplier to select the ion-current corresponding to a given mass, can be driven electronically at a variety of speeds as a means of scanning the mass spectrum. Two such linear ramp circuits are incorporated in the apparatus. In this work, one was usually used to monitor either the primary- or secondary-ion current, while the continuous time-drive feature of the other was used to vary the reaction time t by imposing a continuously varying delay between the electron gate pulse and the ion draw-out pulse via the delay trigger circuitry of a Rutherford type 3-16 pulse generator which supplied the electron gate pulse. At the same time, the ramp voltage generated by the same circuit (necessary to provide the time variation of the pickoff pulse) is used to drive the X axis of an X-Y recorder. Thus, by simultaneously feeding the demodulated primary- or secondary-ion current into the Y-deflection

circuit of the recorder traces of the ion currents as functions of the reaction time are obtained.

Figure 4 shows O^- and NO_2^- ion currents as functions of the reaction time obtained in this way for the reaction



It is worth noting that the sum of the O^- and NO_2^- ion currents is nearly constant for reaction times up to about 1.2 μsec . This indicates that within this time region, there is negligible loss of ions from the reaction region due to their kinetic energy of formation, and that rate constants and cross sections calculated from ion current curves within this region should be accurate. The results presented in this paper were all calculated for such conditions.

D. Gas-Pressure Measurement

Gas pressures in the differentially pumped source region were measured by an MKS Baratron capacitance manometer with a 1-Torr head which had been factory calibrated with a dead weight tester. Pressures used were of the order of 10^{-4} Torr, corresponding to single collision conditions in the source region. The pressures measured by the manometer were checked against a wide-throated calibrated ion gauge connected directly into the source region and against reported ionization cross sections for N_2 and O_2 .¹⁷ In the latter procedure, the electron energy was set at 100 V, and collection of positive ions was made on the electrode normally used to repel negative ions into the flight tube (the backing plate 7 in Fig. 1). The ratio of the positive-ion current to the electron-beam current remained the same to within 4% under normal flow conditions (differential pumping between source region and flight tube) and under static pressure conditions over the range of

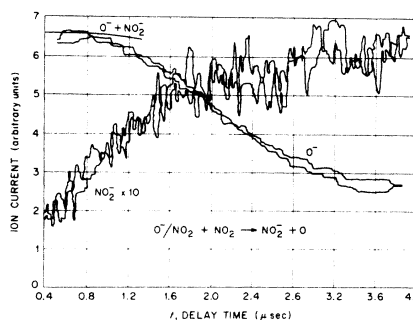


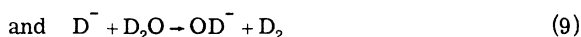
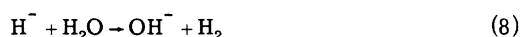
FIG. 4. Modulated components of O^- and NO_2^- ion currents as a function of reaction time t . Two X-Y recorder traces are shown. NO_2 pressure 1.9×10^{-4} Torr.

pressures used in the work reported here. All the pressure measurements described above agreed to within $\pm 5\%$.

III. EXPERIMENTAL RESULTS

Table I lists the reaction rate constants and cross sections obtained in this work with the dissociative attachment resonances used to produce the primary negative ions. Some remarks on each and on some associated reactions follow.

Rate constants for the reactions



measured with the full electron-beam width set at the 6.5 eV main dissociative attachment peak in H_2O and D_2O , have been previously reported.⁸ For D_2O , it has also been possible to make a rate measurement with the full beam width set at the peak of the secondary (8.6 eV) resonance yielding D^- ions of ~ 3.6 eV kinetic energy. In addition, rate constants have now been obtained for reaction (9) by the ordinary constant voltage RPD technique mentioned above at three energies covering the main peak (1.28, 1.84, and 2.32 eV D^- ion kinetic energy).¹⁸ The rate at the peak, 1.84 eV D^- en-

TABLE I. Negative ion-molecule reaction rates and cross sections.

Reaction	Resonance ^a (eV)	Primary-ion energy E (eV) ^b	Rate constant k (molecule ⁻¹ cm ³ sec ⁻¹)	Cross section σ (cm ²)
$\text{H}^- + \text{H}_2\text{O} \rightarrow \text{OH}^- + \text{H}_2$	$\text{H}^-/\text{H}_2\text{O}$ at 6.4	1.9 \pm 0.4	$3.1 \pm 0.6 \times 10^{-8}$	$1.6 \pm 0.3 \times 10^{-14}$
	H^-/H_2 at 14	~ 0	$5.4 \pm 1.6 \times 10^{-7}$	
$\text{D}^- + \text{D}_2\text{O} \rightarrow \text{OD}^- + \text{D}_2$	$\text{D}^-/\text{D}_2\text{O}$ at 8.5	3.6 \pm 0.6	$6.1 \pm 1.2 \times 10^{-8}$	$3.3 \pm 0.7 \times 10^{-14}$
	$\text{D}^-/\text{D}_2\text{O}$ at 6.5	2.3 \pm 0.2		$5.1 \pm 1.0 \times 10^{-14}$
	$\text{D}^-/\text{D}_2\text{O}$ at 6.5	1.8 \pm 0.4	$7.7 \pm 1.5 \times 10^{-8}$	$5.8 \pm 1.2 \times 10^{-14}$
	$\text{D}^-/\text{D}_2\text{O}$ at 6.5	1.3 \pm 0.2		$9.0 \pm 1.8 \times 10^{-14}$
	D^-/D_2 at 14	~ 0	$4.7 \pm 1.5 \times 10^{-7}$	
$\text{O}^- + \text{NO}_2 \rightarrow \text{NO}_2^- + \text{O}$	O^-/O_2 at 6.7	1.6 \pm 0.3	$2.7 \pm 0.3 \times 10^{-9}$	$6.3 \pm 1.2 \times 10^{-15}$
	O^-/NO at 9.3	0.8 \pm 0.2	$3.9 \pm 0.4 \times 10^{-9}$	$1.3 \pm 0.2 \times 10^{-14}$
	$\text{O}^-/\text{N}_2\text{O}$ at 2.6	0.65 \pm 0.05	$2.5 \pm 0.3 \times 10^{-9}$	$9.3 \pm 1.7 \times 10^{-15}$ -2.2
	$\text{O}^-/\text{N}_2\text{O}$ at 2.6	0.48 \pm 0.1	$2.8 \pm 0.3 \times 10^{-9}$	$1.15 \pm 0.2 \times 10^{-14}$
	$\text{O}^-/\text{N}_2\text{O}$ at 2.6	0.41 \pm 0.1	$3.8 \pm 0.7 \times 10^{-9}$	$1.7 \pm 0.4 \times 10^{-14}$
	O^-/NO_2 at 8.8	7.45 \pm 0.1 ^c	$4.4 \pm 0.4 \times 10^{-10}$	
	O^-/NO_2 at 8.8	6.82 \pm 0.1 ^c	$1.0 \pm 0.2 \times 10^{-9}$	
	O^-/NO_2 at 3.8	2.27 \pm 0.1 ^c	$1.8 \pm 0.2 \times 10^{-9}$	
	O^-/NO_2 at 3.8	1.9 \pm 0.1 ^c	$2.4 \pm 0.3 \times 10^{-9}$	
	O^-/NO_2 at 3.8	1.3 \pm 0.1 ^c	$2.4 \pm 0.3 \times 10^{-9}$	
	O^-/NO_2 at 1.9	0.4 \pm 0.1 ^c	$6.6 \pm 0.8 \times 10^{-9}$	
	O^-/NO_2 at 1.9	0.0 \pm 0.1 ^{c, d}	$8.0 \pm 1.0 \times 10^{-9}$	$\geq 4.2 \times 10^{-14}$
O^-/NO_2 at 1.9	-0.25 \pm 0.1 ^c	$4.2 \pm 0.4 \times 10^{-9}$		
$\text{O}^- + \text{N}_2\text{O} \rightarrow \text{NO}^- + \text{NO}$	$\text{O}^-/\text{N}_2\text{O}$ at 2.6	0.65 \pm 0.0 -0.1	$4.0 \pm 0.4 \times 10^{-11}$	$1.5 \pm 0.3 \times 10^{-16}$
$\text{SO}^- + \text{SO}_2 \rightarrow \text{SO}_2^- + \text{SO}$	SO^-/SO_2 ^e at 4.8		$3.7 \pm 1.8 \times 10^{-9}$	
$\text{HCOO}^- + \text{SF}_6 \rightarrow \text{SF}_5^- + (\text{HCOOF})$ ^f	$\text{HCOO}^-/\text{HCOOH}$ at 1.7	~ 0	$\geq 6.0 \times 10^{-8}$ g	
$\text{SF}_6^- + \text{HCl} \rightarrow \text{F}_2\text{Cl}^- + (\text{SF}_4\text{H})$	h	Thermal	$8.6 \pm 2.7 \times 10^{-8}$	

^aDissociative attachment resonance supplying primary ion.

^cElectron energy relative to main, 1.9 eV, O^-/NO_2 peak.

^eIt is possible that there was some contribution from primary O^- ions to this reaction. This is discussed in the text.

^gCalculated with the assumption that the SF_6 pressure was $\leq 10^{-5}$ Torr.

^bPrimary-ion energy (eV) in the laboratory system.

^dPrimary ion energy here was measured to be ≤ 0.25 eV. This yields $\sigma \geq 4.2 \times 10^{-14}$ cm².

^fDenotes SF_5^- excited.

^h SF_6^- from capture of zero energy electrons.

ergy, was a factor of 2.1 lower than the full-beam width measurement. These RPD measurements, however, were regarded as being less reliable in absolute magnitude than the full-beam measurements since they were obtained by a subtraction process involving two small currents. They were therefore normalized to the full-beam measurements⁸ and are thought to give in combination with them a reasonable indication of the trend of the cross section with energy. Because of the high reaction rates and low intensities involved, the studies of reactions (8) and (9) were the most difficult of this work. The low mass of the primary ions also contributed to this since their residence times in the ion source were short as compared with a heavier ion such as O^+ of the same energy.

Rate measurements for these two reactions were also made using H^- and D^- from the ~ 14 V vertical onset dissociative attachment resonance in H_2 or D_2 .¹⁹ For vertical onset processes the potential energy curve of the dissociating state contains a minimum so that only a portion of the ground-vibrational-state wave function of the neutral has an overlap with the dissociating state capable of producing dissociation (that is, only a part falls to the left, low-internuclear-distance side of the minimum). Ions produced in such a way, therefore, have very low energies near zero and their appearance potential curve rises very sharply with a "vertical onset" due to the cutoff caused by the presence of the minimum in the dissociating state.

The method of analysis used in these results was as follows. Normalized H^- and OH^- or D^- and OD^- , currents as a function of reaction time were obtained from the currents observed in the H_2 - H_2O mixture by dividing them by the H^- current observed in H_2 before the addition of the small amount of water vapor. With the assumption that the ion energy distribution is not much changed by the addition of the small quantity of H_2O necessary to observe reaction (8), the normalized H^- current obtained in this way should represent simply the change in H^- concentration with time as a result of reaction (8). Similarly, the normalized OH^- current represents the growth in OH^- concentration with time due to the ion-molecule reaction. This picture is supported by the fact that the H^- and OH^- intensities obtained in this way add to very nearly a constant value over the observable range of reaction times from 0.2 to 1.0 μ sec. However, as seen in Fig. 5, two anomalies occur. Firstly, the sum of the OH^- and H^- currents is not quite constant and increases with reaction time; secondly, the H^- current does not decrease to zero as it is observed to do in the case of the H^-/H_2O resonances,⁸ but levels out at a constant value as the reaction time increases. It is thought that these two facts are both related to the probable presence of a component of H^- ions

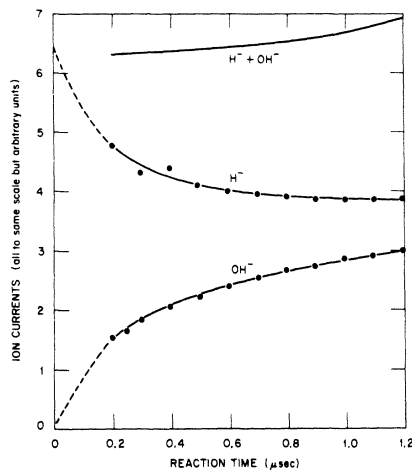


FIG. 5. H^- , OH^- ion currents as functions of the reaction time t for the reaction H^-/H_2 (14-eV peak) $+ H_2O \rightarrow OH^- + H_2$.

of much higher energy than those from the vertical onset process. Both Schulz¹⁹ and Rapp, Sharp, and Briglia¹⁹ observed a continuous rising contribution to the H^- ion current at electron energies above about 12 V. This is quite separate from the discrete vertical onset resonance near 14 eV and may imply the presence of H^- ions of higher energy. If the level portion of the normalized H^- curve at reaction times near 1 μ sec is taken as the zero H^- level, then reaction rates calculated from this curve and from the rising portion of the OH^- curve are in quite good agreement as can be seen in Fig. 6. Because of the low ion intensities and the somewhat speculative nature of this analysis, these results should be used with care. A flowing afterglow measurement of the rate would be valuable.

The distribution of primary H^- or D^- ion energies is difficult to estimate in the vertical onset case. From the electron-beam energy distribution and the shape of the resonance together with the expression (3), a tentative estimate of a mean ion energy of ~ 0.2 eV may be made. Figure 7 shows a plot of the cross sections for the processes (8) and (9) against most probable ion energy. The error bars on the points at ion energies greater than 1 eV represent probable limits of error obtained from a consideration of the uncertainties in the ion energy, the gas pressure, and time and current readings. The points at 0.2-eV ion energy must be regarded with greater caution than the others for the reasons mentioned and should not be taken as being accurate to within better than a factor of ten or so. Paulson²⁰ has obtained rate constants for reaction (9) from a mass spectrometer experiment using repeller voltages constant in time. His results at the lowest repeller voltage are roughly a factor of

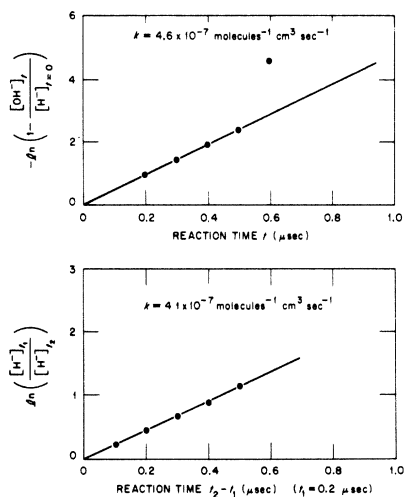


FIG. 6. $\ln([H^-]_t/[H^-]_{t_0})$ and $-\ln(1 - [OH^-]_t/[H^-]_t)$ as functions of the reaction time t for the reaction H^-/H_2 (14-eV peak) + $H_2O \rightarrow OH^- + H_2$. H_2O pressure 3.0×10^{-4} Torr.

20 lower than the present work but since such experiments yield cross sections or rate constants which are averages over a range of ion energies, it is difficult to compare the two experiments. Paulson observed an increase in the rate of the reaction (9) with decreasing repeller voltage implying that the cross section may be increasing faster than $1/v$ (where v is the ion velocity), with decreasing ion energy. This is in qualitative agreement with Fig. 7.

O^- ions of various kinetic energies were produced by dissociative electron attachment to NO_2 ,

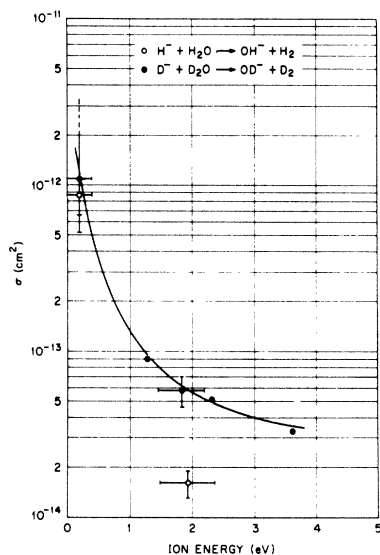


FIG. 7. Cross section σ versus ion energy E for the reactions $H^+ + H_2O \rightarrow OH^- + H_2$ and $D^- + D_2O \rightarrow OD^- + D_2$.

N_2O , NO , and O_2 and were used as primary ions in the study of the exothermic reaction (7). An attempt to use O^- from the 4.4 and ~ 8.0 V dissociative attachment resonances in CO_2 was unsuccessful because of the high O^-/NO_2 levels also produced at these electron energies. Figure 8 shows an X-Y recorder trace of O^-/NO_2 as a function of electron energy obtained using the modulated RPD beam with a width of 0.1 V. Rates for reaction (7) measured at various points along this curve using O^-/NO_2 as the primary ion are also shown. A retarding analysis performed on O^- from the 1.9-eV peak in an apparatus which has been described by Compton, Stockdale, and Reinhardt²¹ was unsuccessful in that it established only that the O^- energy was quite low, probably less than 0.25 eV. Equation (3) indicates that in the absence of vibrational excitation of the NO fragment the most probable O^- kinetic energy at an electron energy of 2.2 eV would be 0.36 eV.

The presence of high scattered-electron currents prevented measurement of O^-/NO_2 kinetic energies at the two higher energy peaks near 3.8 and 8.8 V electron energy. In Sec. IV, it is pointed out that the cross section for an exothermic reaction is expected to rise at least as fast as $1/v$ with decreasing primary ion velocity; therefore, the reaction rate $k = \sigma v$ will either be constant ($1/v$ cross section) or will also increase with decreasing ion energy. The results of Fig. 9 then indicate that the O^- ions from the higher energy peaks in NO_2 are probably formed with higher kinetic energies than those from the first peak; the ions from the 8.8-eV peak with the highest. Knowledge of the dependence of σ on E would, of course, yield these energies. The results of Schulz²² for O^-/N_2O (which have recently been substantiated in part by Dillard and Franklin⁹) and Chantry¹³ for O^-/O_2 were used to obtain ion kinetic energies in these cases. Figure 9 shows a plot of σ against O^- kinetic energy in the laboratory system for reaction (7) obtained in this way. The point at 0.25 eV was found from modulated RPD measurements of the reaction rate using O^-/NO_2 at the lowest-energy dissociative attachment peak on the assumption that the O^- kinetic energy was in fact 0.25 eV. It should, therefore,

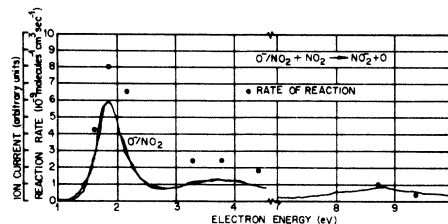


FIG. 8. O^-/NO_2 and the rate constant k for the reaction $O^-/NO_2 + NO_2 \rightarrow NO_2^- + O$ as functions of the electron energy.

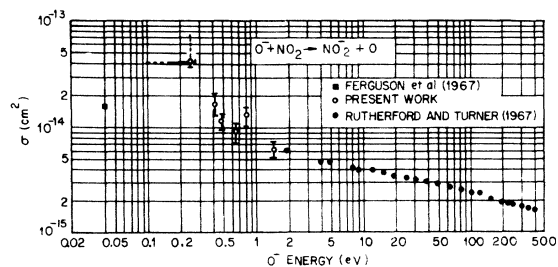


FIG. 9. Cross section σ versus ion energy for the reaction $O^- + NO_2 \rightarrow NO_2^- + O$.

represent a lower limit to the cross section here. The next three points, between 0.4- and 0.7-eV O^- kinetic energy, were obtained using the modulated RPD method to produce O^- from N_2O . The point at 0.8 eV was provided by O^-/NO and that at 1.5 eV by O^-/O_2 . It can be seen that the results of the present work join fairly smoothly onto the retarded beam study of Rutherford and Turner²³ but seem to diverge away from the flowing afterglow results of Ferguson, Fehsenfeld, and Schmeltekopf.²⁴ However, because of the heating of the neutrals in the latter work, it is difficult to compare the flowing afterglow results directly with beam measurements. The beam measurements of Neuert, Rackwitz, and Vogt²⁵ are a factor of 5–10 less than either the present work or the results of Rutherford and Turner²³ over the same range of energies, with the divergence increasing with increasing energy. Paulson²⁰ obtained rates near 1.2×10^{-9} molecules⁻¹ cm³ sec⁻¹ for reaction (7) which compare quite well with the data of Fig. 8 and 9. He observed little change in rate with repeller voltage. By working with pressures as high as 0.2 Torr, Paulson²⁰ was also able to study the reaction



and obtained rates of the order of 1×10^{-11} molecules⁻¹ cm³ sec⁻¹, using O^-/NO_2 from the lowest-energy dissociative attachment peak. O_2^- at this peak energy was at or below the limits of detection in the present work because of the much lower pressures used.

Figure 10 shows the cross section for the reaction



as a function of the O^- -laboratory kinetic energy. O^-/N_2O with a laboratory energy of 0.65 eV was used to obtain the single point from this work. Here the low-energy point is below the extrapolated results of Rutherford and Turner²³ but agrees with the rate obtained by Paulson.²⁰ The reaction

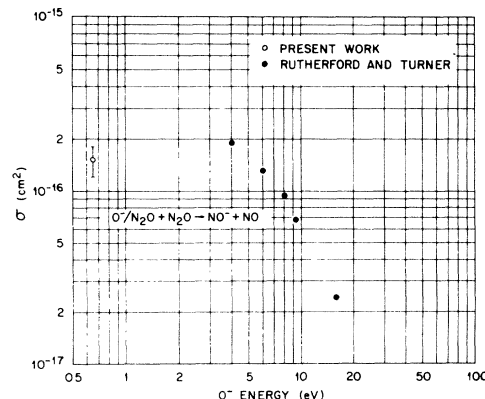


FIG. 10. Cross section σ versus ion energy for the reaction $O^- + N_2O \rightarrow NO^- + NO$.



first proposed by Burt and Henis,²⁶ was not observed. Paulson²⁰ did observe O_2^- but ascribed it to charge exchange of O^- with impurity O_2 . He also noted that N_2O^- and NO_2^- were formed with small rate constants and discussed possible means of formation. Neither were seen in the present work, probably partly because lower pressures were used and partly because the reaction



is endothermic by greater than 0.65 eV and not possible under our conditions with O^-/N_2O .

Melton, Ropp, and Martin²⁷ have reported a rate constant of $\sim 3 \times 10^{-11}$ molecules⁻¹ cm³ sec⁻¹ for the reaction



where $CHOO^-$ is formed by impact of low-energy electrons in the 2–5 eV range in formic acid vapor ($HCOOH$). This is one of a small number of association reactions which have been reported.²⁸ In a careful search in the present work with $HCOO^-/HCOOH$ at 2 eV, no ion of mass 91 was observed, though the sensitivity of the method is such that $HCOOHCOOH^-$ formed at this rate should have been recorded. It is possible that the formation of the complex requires a certain activation energy, and that this was supplied by the repeller field in Melton, Ropp, and Martin's experiment²⁷ but was not available under the field-free conditions of the present experiment. When a small amount of SF_6 was added the SF_5^- ion appeared, and from the time dependences of the $CHOO^-$ and SF_5^- currents it was found that the reaction



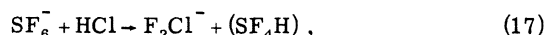
was occurring. Examination of the SF_5^- current in conjunction with a repeller electrode in the flight tube, a technique which has been described by Compton, Hurst, Christophorou, and Reinhardt²⁹ revealed the presence of both charged and neutral components. By varying the ion flight time (changing the bias of the electron multiplier and flight tube above the grounded ion source), the relative magnitudes of the two components could be changed, and the lifetime of the SF_5^- (time for a group of the ions to decay to e^{-1} of their initial number), initially formed in reaction (59), was found to be 3.6 μ sec. The observation of reaction (15) is of interest, since SF_5^- formed by dissociative electron attachment is stable. This seems to be the first case in which the product negative ion of an ion-molecule reaction has been found to decay in this way.

In a mass spectrometric investigation of negative-ion formation, Bailey, McGuire, and Muschlitz³⁰ observed an ion of mass 25 under conditions of low-energy electron impact on CH_4 . They ascribed its formation to a "multiple collision process." Since CH_2^- is formed simultaneously by dissociative attachment, the process



is suggested. Distillation of the CH_4 did not affect the production of the ion of mass 25. A search for mass 25 in the present work, with Phillips's research grade CH_4 , was unsuccessful, though CH_2^- was observed peaking near 5-eV electron energy. The rate of reaction (16) may be low, perhaps energetically forbidden under the circumstances of the present experiment, though biasing the mass spectrometer repeller plate by a few volts negative with respect to the exit slit failed to produce mass 25.

Table I lists one other reaction-rate constant measured in this work, that for the reaction



SF_6^- so formed has a lifetime of 26 μ sec²⁹ so that it was necessary in obtaining the rate to use the rising portion of the F_2Cl^- curve at times short compared with this. Since both SF_6^- and HCl in reaction (17) have the same thermal velocity distribution, conditions here are somewhat similar to the flowing afterglow.

IV. DISCUSSION

A. Energy Dependence of Cross Sections

1. $O^- + NO_2 \rightarrow NO_2^- + O$

The data for this reaction join quite smoothly onto the data of Rutherford and Turner,²³ with

both sets of points being about 5–10 times higher than those of Neuert, Rackwitz, and Vogt.²⁵ This discrepancy increases towards higher primary-ion energies. Though Neuert, Rackwitz, and Vogt do not discuss the energy resolution of the ion beam used in their apparatus, it should be adequate at least at energies near 200 eV. There seems then to be no clear reason for such a large discrepancy. Turner and Wolf³¹ have fitted the Rutherford and Turner data and the low-energy flowing afterglow point of Ferguson, Fehsenfeld, and Schmeltekopf²⁴ to a semiempirical theory which trends towards the Langevin³² $E^{-1/2}$ cross section for capture of an ion in a r^{-4} potential¹⁴ at low energies and towards the expression for symmetric resonant charge-transfer ($\sigma = c - d \log_{10} E$, where c and d are constants)³³ at high energies. They obtain a good fit over the energy range from 0.04 to 100 eV using a single adjustable parameter. Neuert, Rackwitz, and Vogt²⁵ have also fitted their data to the symmetric resonant charge-transfer theory using two separate straight lines with different values of the constants c and d to cover the two energy ranges: 3.0–20.0 eV and 20–200 eV. The fit in the low-energy region in this case is not particularly good, and no discussion of the procedure is given. There does not seem to be any clear theoretical justification for it. Nevertheless, it is of interest that the cross section rises towards lower ion energies, a fact agreed on by all the measurements. This means that the Ropp and Francis³⁴ theory of asymmetric nonresonant charge exchange certainly cannot be applied, since it predicts a cross section rising sharply towards higher energies, roughly as E^2 , for the low-energy region. The apparent similarity between the form of the cross section and that of low-energy exothermic ion-molecule reactions also tends to confirm the recent suggestion of Champion and Doverspike³⁵ that low-energy ion-molecule and charge-exchange reactions proceed in a similar way.

The four higher-energy points obtained in the present study do not show any significant deviation from the theory of Wolf and Turner³¹ (for which the best fit is virtually a linear interpolation between the flowing afterglow point and the data of Rutherford and Turner).²³ However, the two lowest-energy points, in particular the one at 0.25 eV, diverge from this trend and disagreement with this theory and with the $E^{-1/2}$ Langevin dependence at low energies seems quite possible. If the O^-/NO_2 kinetic energy for the lowest-energy point is taken as 0.36 eV as calculated from Eq. (3) a cross section of 3.9×10^{-14} cm² is obtained and the deviation remains. Figure 11 shows the data points for this work plotted against E^{-1} and $E^{-1/2}$. Though obviously more data at low energies are needed, the results tend to favor the E^{-1} rather than $E^{-1/2}$ energy dependence. Accurate measurements of the kinetic energies of the

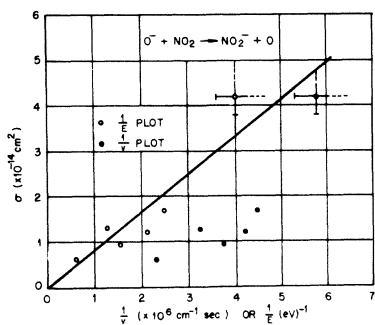


FIG. 11. Cross section σ versus E^{-1} and $1/v$ for the reaction $O^- + NO_2 \rightarrow NO_2^- + O$.

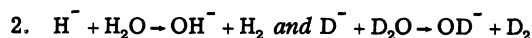
O^- ions produced by dissociative electron attachment to NO_2 would be valuable, since these would permit calculation of cross sections from the rates shown in Fig. 8. Dugan and Magee^{36,37} have performed numerical integration of the classical Lagrange equations to obtain particle trajectories for a number of molecules which possess a γ^{-2} permanent dipole potential as well as the γ^{-4} induced dipole of the Langevin theory. They have not reported an estimate of the dependence of the cross section on energy for NO_2 , but probably the prediction would be for a dependence of $\sim(E^{-1})^{0.7}$ at these energies. A Stark effect calculation for unhindered rotation made by the same authors³⁶ does predict a E^{-1} dependence, but for this model to be valid, the reaction would have to occur at distances greater than that at which the free rotation of the NO_2 begins to be hindered by the approach of the O^- ion (i. e., at distances greater than about 30 Å). This is implausible on the basis of the classical orbit calculations^{36,37}; however, Bohm, Hasted, and Ong³⁸ have obtained best agreement with a number of experimental thermal energy ion-molecule reaction rates by using a value of 100 Å for the adiabatic parameter a in an application of Massey's adiabatic criterion³⁹ to ion-molecule reactions.

The measured cross sections for reaction (7) are composites of reactions with NO_2 of O^- ions in the two possible J states $^2P_{3/2}$ and $^2P_{1/2}$ from the ground-state configuration $1s^22s^22p^5$ of O^- . Since the highest energy point in the present work (O^-/O_2 at 6.5 eV) is in good agreement with the lowest-energy point of Rutherford and Turner,²⁵ where the O^- was produced in an entirely different higher-energy electron-bombardment source, and since, even at 6.5 eV, the ionizing electron in the dissociative attachment process may have considerable angular momentum it seems likely that in both experiments the O^- was formed in the $^2P_{1/2}$ and $^2P_{3/2}$ states in proportions corresponding to the statistical weights M_J , that is, 2 and 4, respectively, for the two states. Of course, other possibilities, equal proportions but not according to the

statistical weights, and/or cross section independent of the input ion state cannot be ruled out but are perhaps less likely.

For the case of O^-/O_2 , the kinetic energies of the O^- ions in the two states are within about 0.03 eV, since the J splittings are quite small for O^- and for the neutral O, which is produced in 3P_0 , 3P_1 , 3P_2 states.⁴⁰ Similar remarks might be made for the O^- ions produced by the other dissociative attachment processes.

It is known that over-all spin conservation is not a necessary condition for a fast ion-molecule reaction, but it is likely that spin conservation is required in the formation of a complex. Strong coupling after the complex is formed could lead to spin breakdown, but $\vec{J} = \vec{L} + \vec{S}$ should be conserved (\vec{L} is not), and it might be possible to use spin-orbit coupling.² Plainly, there is need for quantum-mechanical studies of low-energy ion-molecule reactions coupled with experimental work using state selected ion beams. The possibility exists that the deviation of the lower energy points in the present results from a near $E^{-1/2}$ dependence may be due to a change in the relative numbers or reaction rates of the two kinds of O^- ions present.



There are no other experimental cross-section data for direct comparison with the results of Table I. Most of the information on the variation of the cross section with energy is from the study of the second of these two reactions, though they both appear to have a similar trend. Figure 12 shows σ plotted against E^{-1} and $E^{-1/2}$ for the second reaction, and as for the reaction (7), the E^{-1} dependence is favored. Dugan⁴¹ has obtained an energy dependence of $(E^{-1})^{0.65}$ for ion collisions with H_2O and D_2O from numerical integration of the Lagrange equations. The comments made in the preceding paragraphs on the variation of cross section with energy apply again here though these are obviously ion-molecule reactions.⁴² It is

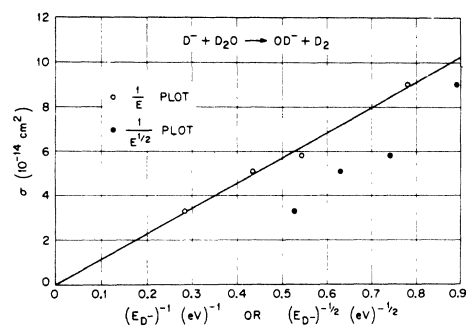


FIG. 12. Cross section σ versus E^{-1} and $E^{-1/2}$ for the reaction $D^- + D_2O \rightarrow OD^- + D_2$.

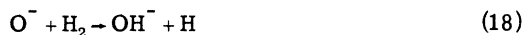
worth remarking that Moran and Hamill⁴³ have reported cross-sectional dependence near E^{-1} in mass spectrometer studies of ion-molecule reactions of CH_3CN^+ and $\text{C}_6\text{D}_{12}^+$ ions with the symmetric top molecule CH_3CN .

3. $\text{O}^- + \text{N}_2\text{O} \rightarrow \text{NO}^- + \text{NO}$

The single point (at an O^- energy of 0.65 eV) obtained in the present work appears to be somewhat below the extrapolated data of Rutherford and Turner²³ but agrees well with the rate reported by Paulson.²⁰ This reaction is obviously of interest, but in the absence of further low-energy data speculation seems inadvisable.

B. Isotope Effect

The ratio of the cross sections $\sigma_{(9)}/\sigma_{(8)} = 3.6$ at 1.8 eV is surprisingly high. Normalizing the results to equal primary-ion velocities only reduces this ratio by about 30%. The classical orbiting calculations of Dugan and Magee^{36,37} and Dugan, Rice, and Magee⁴⁴ predict that the cross section is insensitive to the moment of inertia of the target molecule and do not appear capable of explaining this result. Martin and Bailey⁴⁵ have reported a similar large isotope effect in a low-energy beam study of the reactions



but were also unable to explain the isotope effect in terms of existing theory.

The Langevin theory³² predicts an opposite and much smaller isotope effect to that observed in both these studies. The semiclassical theory of Dugan and Magee,³⁶ which employs the Stark effect, also does not seem to provide an explanation for the present data, since the first-order term, which is expected to be dominant, does not contain the molecular moments of inertia and the average over the rotational quantum numbers which is involved in the calculation is expected to be similar for the two reactions (8) and (9).

C. Upper Limits to Cross Sections

The results listed in Table I are within the limits of a calculated maximum cross section made by Dugan and Magee⁴⁶ except for the rates for reactions (8) and (9) using "zero energy" H^-/H_2 and D^-/D_2 ions from the ~ 14 eV vertical onset resonances, which are roughly a factor of 10 higher than the theory predicts for a primary-ion energy of 0.2 eV. In view of the uncertainties in the primary-ion energy and in the calculation of the maximum cross section, this disagreement is not felt

to be serious. A point which is of interest is the participation of high angular momenta (in units of \hbar) in these collisions, permitting large cross sections. For instance, in the case of a 2-eV H^- ion, with impact parameters of up to 4 Å in a collision with H_2O , l_{max} , the maximum angular momentum, is 120 \hbar . The maximum reaction cross section is given by Blatt and Weisskopf⁴⁷ to be

$$\begin{aligned} \sigma_{\text{max}} &= \sum_{l=0}^{l_{\text{max}}} \pi \kappa^2 (2l+1) \\ &\approx \pi \kappa^2 l_{\text{max}}^2, \quad \text{for large } l_{\text{max}}, \end{aligned} \quad (20)$$

which gives $\sigma_{\text{max}} \approx 10^{-14}$ cm² for $l_{\text{max}} = 120 \hbar$, the higher angular momenta being dominant in this result.

ACKNOWLEDGMENTS

The authors are indebted to Dr. J. F. Burns, Dr. H. C. Schweinler, Dr. C. E. Klots, Dr. W. R. Garrett, and Dr. J. E. Turner of this laboratory and the University of Tennessee for stimulating discussions of a number of points in this paper. Dr. J. V. Dugan of NASA Lewis Research Center kindly sent us before publication the results of his calculations on the energy dependence of the cross sections of the reactions (8) and (9).

APPENDIX

The effect of the finite timewidth of the electron gate pulse may be allowed for the following unfolding technique.

The time dependence of the product-ion current i_S for a negligibly small electron gate pulse width is of the form

$$i_S = A(1 - e^{-B(t-t_0)}), \quad (21)$$

where A , B , and t_0 are constants. This follows from Eq. (4) where t_0 is introduced here to permit the possibility of a small translation in the time axis between the experimentally measured curves and the unfolded curve (21).

Since the electron gate is a square pulse of time width δ the time dependence of the observed secondary current I_S is given by

$$I_S(x) = \frac{1}{\delta} \int_{x-w_1}^{x+w_2} A(1 - e^{-B(t-t_0)}) dt, \quad (22)$$

where the experimental time variable is now denoted by x . The factor $1/\delta$ necessary for normal-

ization and the limits of integration are taken from $x - w_1$ to $x + w_2$, where $w_1 + w_2 = \delta$ to permit an arbitrary choice of centering of the electron gate pulse about a given experimental time point x . Integration of (22) results in the expression

$$I_S(x) = \frac{1}{\delta} \left[A(w_2 + w_1) + A \frac{e^{-Bx} e^{-Bt_0}}{B} \times (e^{-Bw_2} - e^{-Bw_1}) \right] \quad (23)$$

The experimental points are compared with this expression over the range of times x in which the sum of the observed primary- and secondary-ion currents is constant. The constants A , B , and t_0 are then calculated by a digital computer programmed to select A , B , and t_0 , so that the sum of the squares of the residuals of the experimental and theoretical [from Eq. (23)] points is minimized. In general, this unfolding procedure had a small effect on the data reported here, changing the first estimates of the reaction rates by $\lesssim 10\%$.

[†]Research sponsored by the U. S., Atomic Energy Commission under contract with Union Carbide Corporation.

¹D. S. Burch and R. Geballe, *Phys. Rev.* **106**, 188 (1957); H. Eiber, *Z. Angew. Phys.* **15**, 103 (1963); E. C. Beaty, L. M. Branscomb, and P. L. Patterson, *Bull. Am. Phys. Soc.* **9**, 535 (1964); J. L. Moruzzi and A. V. Phelps, *J. Chem. Phys.* **45**, 4617 (1966); J. L. Moruzzi, J. W. Ekin, Jr., and A. V. Phelps, *ibid.* **48**, 3070 (1968).

²E. E. Ferguson, *Advan. Electron. Electron Phys.* **24**, 31 (1968).

³W. L. Fite, R. T. Brackman, and W. R. Snow, *Phys. Rev.* **112**, 1161 (1958); W. L. Fite, A. C. H. Smith, and R. F. Stebbings, *Proc. Roy. Soc. (London)* **A268**, 527 (1962); R. F. Stebbings and J. A. Rutherford, *J. Geophys. Res.* **73**, 1035 (1968); J. H. Simons, H. T. Francis, C. M. Fontana, and S. R. Jackson, *Rev. Sci. Instr.* **13**, 419 (1952); E. E. Muschlitz, *Phys. Rev.* **95**, 635 (1954).

⁴If the nature of the experiment permits its operation within a magnetic field and if mass resolution in the analysis of beam impurities is not important, velocity analyzing the beam at the low energy at which it is finally required does permit the production of 1–3-eV ion beams with an energy spread of ~ 0.25 eV. P. H. Edmonds and J. B. Hasted, *Proc. Phys. Soc. (London)* **84**, 99 (1964).

⁵S. M. Trujillo, R. H. Neynaber, and E. W. Rothe, *Rev. Sci. Instr.* **37**, 1655 (1966); V. A. Belyaev, B. G. Brezhnev, and E. M. Erastov, *Zh. Eksperim. i Teor. Fiz. Pis'ma v Redaktsiyu* **3**, 321 (1966) [English transl.: *Soviet Phys. - JETP Letters* **3**, 207 (1966)]; R. H. Neynaber and S. M. Trujillo, *Phys. Rev.* **167**, 63 (1968).

⁶A. L. Schmeltkopf, F. C. Fehsenfeld, G. I. Gilman, and E. E. Ferguson, *Planet Space Sci.* **15**, 401 (1967); R. F. Stebbings, B. R. Turner, and J. A. Rutherford, *J. Geophys. Res.* **71**, 771 (1966).

⁷Listings of much of this work are given by J. H. Futrell and F. P. Abramson, *Advan. Chem.* **58**, 107 (1966).

⁸J. A. D. Stockdale, R. N. Compton, and P. W. Reinhardt, *Phys. Rev. Letters* **21**, 664 (1968).

⁹J. G. Dillard and J. L. Franklin, *J. Chem. Phys.* **48**, 2349 (1968); **48**, 2343 (1968).

¹⁰J. G. Dillard, J. L. Franklin, and W. A. Seitz, *J. Chem. Phys.* **48**, 3828 (1968).

¹¹R. N. Compton, R. H. Huebner, P. W. Reinhardt, and

L. G. Christophorou, *J. Chem. Phys.* **45**, 4634 (1966).

¹²L. G. Christophorou and J. A. Stockdale, *J. Chem. Phys.* **48**, 1956 (1968).

¹³P. J. Chantry, *Phys. Rev.* **172**, 125 (1968).

¹⁴J. L. Franklin, P. M. Hierl, and D. A. Whan, *J. Chem. Phys.* **47**, 3148 (1967).

¹⁵R. E. Fox, W. M. Hickam, D. J. Grove, and T. Kjeldaa, Jr., *Rev. Sci. Instr.* **26**, 1101 (1955).

¹⁶P. J. Chantry and G. J. Schulz, *Phys. Rev. Letters* **12**, 449 (1964); *Phys. Rev.* **156**, 134 (1967).

¹⁷J. T. Tate and P. T. Smith, *Phys. Rev.* **39**, 270 (1932); R. K. Asundi, J. D. Craggs, and M. V. Kurepa, *Proc. Phys. Soc. (London)* **82**, 967 (1963); B. L. Schram, H. R. Moustafa, J. Schutten, and F. J. DeHeer, *Physica* **32**, 734 (1966).

¹⁸G. J. Schulz, *J. Chem. Phys.* **33**, 1661 (1960).

¹⁹G. J. Schulz, *Phys. Rev.* **113**, 816 (1959); D. Rapp, T. E. Sharp, and D. D. Briglia, *Phys. Rev. Letters* **14**, 533 (1965).

²⁰J. F. Paulson, *Advan. Chem.* **58**, 28 (1966).

²¹R. N. Compton, J. A. Stockdale, and P. W. Reinhardt, *Phys. Rev.* **180**, 111 (1969).

²²G. J. Schulz, *J. Chem. Phys.* **34**, 1778 (1961).

²³J. A. Rutherford and B. R. Turner, *J. Geophys. Res.* **72**, 3795 (1967).

²⁴E. E. Ferguson, F. C. Fehsenfeld, and A. L. Schmeltkopf (private communication) reported in Ref. 34.

²⁵H. Neuert, R. Rackwitz, and D. Vogt, *Advan. Mass. Spectrometry* **4**, 631 (1968).

²⁶B. P. Burt and J. Henis, *J. Chem. Phys.* **41**, 1510 (1964).

²⁷C. E. Melton, G. A. Ropp, and T. W. Martin, *J. Am. Chem. Soc.* **64**, 1577 (1960).

²⁸C. F. Giese, *Advan. Chem. Phys.* **10**, 247 (1966); see also Ref. 2.

²⁹R. N. Compton, G. S. Hurst, L. G. Christophorou, and P. W. Reinhardt, *J. Chem. Phys.* **45**, 4634 (1966).

³⁰T. L. Bailey, J. M. McGuire, and E. E. Muschlitz, *J. Chem. Phys.* **22**, 2088 (1954).

³¹F. A. Wolf and B. R. Turner, *J. Chem. Phys.* **48**, 4226 (1968).

³²P. Langevin, *Ann. Chim. Phys.* **5**, 245 (1905). For application of this theory to ion-molecule reaction studies see G. Gioumousis and D. P. Stevenson, *J. Chem. Phys.* **29**, 294 (1958).

³³M. S. W. Massey and R. A. Smith, *Proc. Roy. Soc.*

(London) *A142*, 142 (1933); B. M. Smirnov, *Teplofizika Vysokiken Temperatur* **4**, 429 (1966) [English transl.: *Soviet Phys. - High Temp.* **4**, 407 (1966)].

³⁴D. Rapp and W. E. Francis, *J. Chem. Phys.* **37**, 2361 (1962).

³⁵R. L. Champion and L. D. Doverspike, *J. Chem. Phys.* **49**, 4321 (1968).

³⁶J. V. Dugan and J. L. Magee, *J. Chem. Phys.* **47**, 3103 (1967).

³⁷J. V. Dugan and J. L. Magee, *Bull. Am. Phys. Soc.* **14**, 261 (1969).

³⁸D. K. Bohme, J. B. Hasted, and P. P. Ong, *Chem. Phys. Letters* **1**, 259 (1967); *J. Phys. B* **1**, 879 (1968).

³⁹H. S. W. Massey, *Rept. Progr. Phys.* **12**, 248 (1949).

⁴⁰L. M. Branscomb, D. S. Burch, S. J. Smith, and S. Geltman, *Phys. Rev.* **111**, 504 (1958).

⁴¹J. V. Dugan (private communication).

⁴²J. F. Paulson (Ref. 22) attempted by using O⁻ from dissociative attachment to O₂¹⁸ to establish whether re-

action (7) proceeds by direct charge exchange or by ion-atom interchange but was unsuccessful because of isotopic exchange in the sample reservoir.

⁴³T. F. Moran and W. H. Hamill, *J. Chem. Phys.* **39**, 1413 (1963).

⁴⁴J. V. Dugan, J. H. Rice, and J. L. Magee, NASA Tech. Memorandum X-1586, 1968 (unpublished).

⁴⁵J. D. Martin and T. L. Bailey, *J. Chem. Phys.* **49**, 1977 (1968).

⁴⁶This calculation is described in Ref. 36. It is based on the argument that, for a molecule with a permanent electric dipole moment, the maximum reaction cross section will result if the dipole continually orients itself to the incoming ion so that the angle between the dipole axis and the radius vector remains zero throughout the interaction.

⁴⁷J. M. Blatt and V. F. Weisskopf, *Theoretical Nuclear Physics* (Wiley-Interscience, Inc., New York, 1962), p. 321.

Density Effect in Equilibrium Charge-State Distributions

G. Ryding, A. Wittkower, and P. H. Rose

R. J. VandeGraaff Laboratory, High Voltage Engineering Corporation, Burlington, Massachusetts 01803

(Received 3 April 1969)

Cross sections for single and multiple electron capture and loss have been measured for iodine ions in hydrogen at 4.50 MeV. Values were determined from the initial behavior of charge-fraction growth curves under thin-target conditions. Equilibrium charge-state fractions F_i were then calculated from the measured cross sections, and these values were compared with the fractions measured directly in a dense target. It is concluded that when multiple collisions occur, excited states in the projectile influence the effective charge-changing cross sections. Consequently measured values of the "equilibrium" charge-state fractions depend in a complex way upon the excited-state lifetimes and the target density. In this experiment, the mean charge calculated from cross-section values was 1.98, whereas, the measured mean charge was 2.33.

INTRODUCTION

The charge of a fast ion moving through matter fluctuates as a result of electron loss and capture in collisions with the stationary atoms of the target. After a sufficient number of collisions, an equilibrium distribution of charges is established which is dependent only on the velocity of the ions and the nature of the target. The effect of the density of the target material upon the charge distribution was first observed by Lassen¹ who measured the mean charge of uranium fission fragments traversing thin-metal films and gases. He found that the mean charge in gases increased by ~16% as the gas pressure

was increased, and that the mean charge in foils was substantially greater than that in gases.

Bohr and Lindhard² were the first to suggest that this increase in the mean charge \bar{i} with target density is a result of an increased probability for the loss of electrons from excited states. In gases at very low pressures, when the lifetime of the excited states is much less than the time between successive collisions, the mean charge is independent of the density. As the density is increased, however, the time between collisions becomes comparable to the lifetime of excited states and an increase in mean charge is to be expected. Bohr and Lindhard estimated the magnitude of this increase to be ~20%. They